Journal of *Marine Science and Engineering*

MDPI

Article

Research on Structural Response Characteristics of Trapezoidal Floating Body in Waves

Xuemin Song [1,2], Weiqin Liu [1,2,*] and Guowei Zhang [2]

[1] Key Laboratory of High Performance Ship Technology, Wuhan University of Technology Ministry of Education, Wuhan 430070, China
[2] School of Naval Architecture, Ocean and Energy Power Engineering, Wuhan University of Technology, Wuhan 430070, China
* Correspondence: liuweiqin_123@sina.com; Tel.: +86-135-5427-4050

Abstract: Floating structures plays an important role in extending and developing ocean resources, and their response evaluation is a hot topic of global important research due to the large dimensions. With characteristics including small depth and large horizontal plane, it is easy to induce the hydro-elastic resonant responses due to total stiffness. In this paper, first, the model design is performed to satisfy hydro-elastic similarity. Then, the model test is carried out in a wave tank to measure the structural response of a trapezoidal floating body in a series of waves. Secondly, the 3D hydro-elastic computational platform HOMER is applied to calculate the stress response of a trapezoidal floating body in numerical waves. The model test results and numerical simulation results are analyzed and compared and the conclusions are drawn, which indicate that a numerical method is effective to predict the structural response characteristics of a trapezoidal floating body. Above all, it is found that the significant response of a floating model is generated in some cases. The methods and conclusions of this study are used to provide reference and guidance for structural design of a trapezoidal floating body.

Keywords: trapezoidal floating body; model test; numerical calculation; load; stress; hydro-elastic response

Citation: Song, X.; Liu, W.; Zhang, G. Research on Structural Response Characteristics of Trapezoidal Floating Body in Waves. *J. Mar. Sci. Eng.* **2022**, *10*, 1756. https://doi.org/10.3390/jmse10111756

Academic Editor: Rodolfo Trentin Gonçalves

Received: 21 September 2022
Accepted: 8 November 2022
Published: 15 November 2022

1. Introduction

With the construction on islands and reefs and the continuous development of resources, the scattered distribution of islands and reefs and the narrow land area cannot support the rapid construction and development. The development and exploration of marine resources has become an important direction for the development and protection of humans. In order to do this, it is necessary to construct long-term platforms in the far out to sea which integrate the comprehensive functions of cruise ship docking, living and entertainment. Therefore, the idea of large floating bodies was developed. Compared with ordinary ships, large floating bodies have a huge volume and wide area, which can carry huge equipment and rich life materials [1].

Large floating bodies demonstrate a variety of application prospects, such as maritime airports, fishing grounds, replenishment stations, marine repair shops, resorts, etc. The mobile marine base of the United States is a semi-submersible large floating body, which is composed of several modules. It can be used as a runway for the takeoff and landing of shipboard aircraft, as well as for the docking and supply of passing ships, and is mostly used in offshore or international waters [1]. The box-type large floating body is a major type of large floating structure. It is composed of floating boxes on the sea surface. The large floating structure, after splicing, is similar to a flat plate and can be used as a runway for aircraft takeoff and landing, or as a container terminal [2,3]. Mega-float is a typical representative of a large box-type floating body. The sea airstrip at Osaka Kansai International Airport also uses a large box-type floating body. China has also made some developments in the design of large floating bodies, among which Shanghai Jiao Tong University and China National Offshore Oil Corporation jointly designed a large

floating offshore base (VLFOB) [4]. China Shipbuilding Industry Corporation also exhibited China's first super-large floating body in the national defense science, technology, industry integration development achievements conference [5].

The evaluation of load and response is one of the main problems in the design process of large floating structures. One of the feasible ways to study the load and response of large floating bodies is model tests. Yago et al. [6,7] conducted model tests of multi-module ultra-large floating bodies to test the response of floating bodies under rigid and flexible connections. Wu Sheng et al. [8] launched a series of large-scale floating body model tests near islands and reefs, also taking into account the complex seabed topography near islands and reefs. Chen Guojian et al. [9] designed a box-shaped ultra-large floating body model, bonded by a foam material layer and thin metal plate, and carried out a hydro-elastic response model test for the box-shaped ultra-large floating body model in a wave tank, mainly to test the deformation and displacement of the ultra-large floating body. Wan Zhinan et al. [10] carried out a series of hydro-elastic model tests of a large box-shaped floating body in different water depth and wave length, and analyzed the hydro-elastic response of the hydro-elastic model, it provided the guidance for further research.

The three-dimensional hydro-elastic numerical method can be used to analyze the complex loads and responses of large floating bodies due to hydro-elasticity. Bishop and Price proposed a two-dimensional beam hydro-elastic theory based on potential flow theory and modal superposition method to evaluate the linear hydro-elastic response of hull beams [11]. Wu Yousheng proposed the three-dimensional hydro-elasticity theory and method in the 1980s, and used a three-dimensional finite element method to calculate the response of ship hull under waves [12]. Ohkusu et al. used the three-dimensional hydro-elasticity theory to consider diffraction and radiation velocity potential, and used dry mode for superposition to obtain structural deformation [13]. Hamamoto used the wet modal method to study the hydro-elastic response and calculate the added mass of the plate in the water [14]. Mamidipudi first applied the three-dimensional hydroelasticity theory to calculate the hydro-elasticity of VLFS, and used the finite central difference method to solve the coupled hydro-elasticity governing equation [15]. Malenica used a three-dimensional hydro-elastic software named HOMER to model and solve the ship structure, the linear vibration and hydro-elastic response of the ship structure under the linear wave were obtained [16]. Lu Ye analyzed the three-dimensional hydro-elastic motion response of the floating platform based on THAFTS software, and obtained the overall stress distribution of the floating platform near the islands and reefs. The results showed that the layout of the floating platform near the islands and reefs must consider the influence of non-uniform seabed topography [17]. Zhang Guowei used HOMER to calculate the hydro-elastic response of a trapezoidal large floating structure [18]. Yang Peng and Gu Xuekang established the coupled hydrodynamic model of floating body and reef by using the boundary element method based on Green's function, and carried out the coupled response analysis of floating body and topography [19]. Based on the three-dimensional finite element method, Gu Xuekang analyzed the total vibration mode of the module in vacuum, and calculated the resonance and modal response of the module in the flow field by combining the modal superposition method and boundary element method [20]. Ding Jun and Tian Chao et al. established the coupled model for the direct analysis of the hydrodynamic performance of floating bodies near the reef and compiled the relevant program THAFTS-BR based on the water wave model and Rankine source method [21]. Tian Chao and Ding Jun et al. used the gentle slope equation to consider the impact of the wave environment near the island and proposed a calculation method for predicting the wave motion and load response of semi-submersible platform near the island [22]. Selvan et al. [23–25] studied the hydro-elastic response of floating structure by numerical method and the conclusions were drawn to guide the design of the structure. Behera et al. [26] presented analytical study for oblique wave scattering by a floating elastic plate in a one or two-layer body of water over a porous seabed of infinite depth; the results were useful in the design of breakwaters.

A trapezoidal floating body is designed as a far-reaching sea support platform for docking, replenishment and simple maintenance of passing ships, law enforcement ships, fishing boats, etc. Due to the design and usage requirements, the horizontal shape of the trapezoidal floating body presents a trapezoidal shape. The depth is smaller than that of the horizontal scale, and presents the characteristics of wide and flat shape. Therefore, the overall stiffness is low and may easily cause a natural vibration response. There is a big difference between the wide flat shape and the long beam-shaped ship structure, and the deformation is no longer the only two-node vibration mode, so the horizontal deformation under complex load is worth studying. In this paper, the test model is designed according to the similarity theory in Section 2; it is similar to the foam layer of materials and the design of sheet metal bonding trapezoidal structure model of the floating body by Chen guo-jian [9]. In Section 3, the three-dimensional hydro-elastic platform HOMER Simpson numerical simulation analysis is carried out on the trapezoidal floating body model, the model test results compared with the results of numerical simulation, based on the results of time domain and frequency domain analysis, the structure stress distribution and frequency domain of the trapezoidal floating body model and time domain response characteristics, are obtained. Above all, the evaluation of structural strength and guidance of the engineering design of prototype structure is provided.

2. Model Test for Load and Response of Trapezoidal Floating Body Model

2.1. Model Design of Trapezoidal Floating Body

The trapezoidal floating body model is a scale model of a large floating body. The model is designed to study the load and response characteristics of the trapezoidal floating body. The model needs to meet the requirements of geometric similarity, hydrodynamic similarity and structural stiffness similarity [8].

Geometric similarity means that the main scale, deformation, wavelength and wave height of the real trapezoidal floating body and the model should all perform a scale ratio relationship, as shown in Equation (1), where L is the main scale and λ is the scale ratio, the subscript r represents the full scale structure, and m represents the model.

$$\frac{L_r}{L_m} = \lambda \tag{1}$$

With consideration of the influence of free surface and gravity, hydrodynamic similarity requires that the Froude number of the full scale structure and the model must be equal. In addition, waves with periodic movement are regarded as unsteady flow, so the Strouhal number must be equal between real waves and waves in tank, and the formula can be obtained as Equation (2) [23].

$$\frac{v_r}{\sqrt{g_r L_r}} = \frac{v_m}{\sqrt{g_m L_m}}, \frac{L_r}{v_r T_r} = \frac{L_m}{v_m T_m} \tag{2}$$

where v is the velocity, T is the wave period and g is the acceleration of gravity. According to the structural stiffness similarity, the relationship between the load stiffness ratio of the full model and the model is obtained based on the deformation of the full model and the model, as shown in Equation (3).

$$\frac{w_r}{w_m} = \lambda, \frac{Q_r L_r^3}{E_r I_r} = \lambda \frac{Q_m L_m^3}{E_m I_m} \tag{3}$$

where, w is the deflection of the object and Q is distributed loads on the surface. The loads of full model and model show a cubic relation of scale ratio. The stiffness relation between full model and model can be obtained by Equation (4) [24].

$$\frac{E_r I_r}{E_m I_m} = \lambda^5 \tag{4}$$

The trapezoidal floating body model for model tests is designed according to the geometric similarity, dynamic similarity and structural static similarity theory. The geometric scale ratio of the model is determined in consideration of the scale of wave tank and the wave-height of the wave-maker. The main scale of the full model and the model is shown in Table 1. The design also meets the hydrodynamic similar wave condition.

Table 1. Main Dimensions of Trapezoidal VLFS Model.

Principal Dimension	Full Model/*m*	Model/*m*
Length in long side (L)	222	2.22
Length in short side (S)	176	1.761
Width	40	0.400
Depth	10	0.100
Draft	3	0.030

In order to meet the structural static similarity between the model and the full model, the structural scheme of the large floating body model is constructed. Firstly, the similar stiffness relation between the model and the full model should be guaranteed to meet the Equation (4); the shape is consistent with the full model which is a trapezoidal shape as shown in Figure 1. The sandwich structure is adopted for model design as described in Figure 2, the structure is composed of waterproof foam layer and steel plate; the foam layer provides drainage volume and buoyancy and the steel plate provides strength and places of strain measurement. The thickness of steel plate should meet the similarity relation Equation (4). During the model test, ballast irons are placed on the plate to ensure that the designed draft is reached.

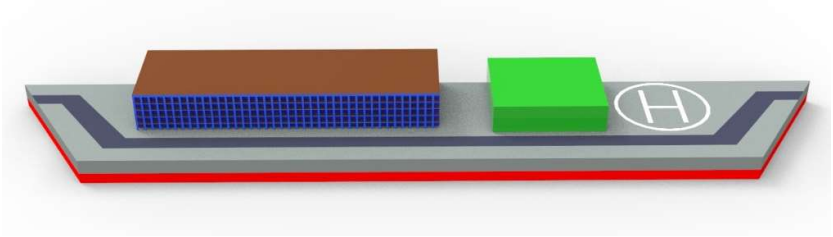

Figure 1. Schematic diagram of full scale structure.

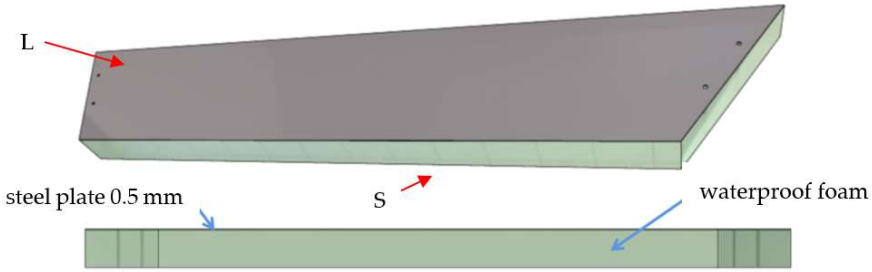

Figure 2. Schematic diagram of model.

2.2. Trapezoidal Floating Body Model Test Conditions

In this study, the model should be elastic to be measured for strain information. A two-layer structure is used for the experiment model, as Figure 2 shows; the upper layer is 0.5 mm steel plate, which can be measured by strain gage, and the under layer is 100 mm waterproof foam material with low hardness, which can provide buoyancy and initial stiffness. The steel plate and foam layer are connected by super glue to constitute a trapezoidal floating body model. Most of the model is made of the foam layer, with a water immersion mass of about 4.8 kg, a draft of 30 mm and a displacement of about 23.9 kg. In order to achieve the target draft, the displacement is increased by arranging the ballast iron in the test, and a total of 19.4 kg of ballast iron is used. Four three-way dynamic

strain gauges are arranged on the steel plate of the trapezoidal floating body model for recording the dynamic deformation signals of the model under waves as shown in Figure 3. In order to study the stress response characteristics of the trapezoidal floating body model in different waves, the responses under three wave direction angles of −30°, 0° and 30° are experimentally tested as displayed in Figure 2. The wave frequency range of each wave is from 0.1 rad/s to 15 rad/s. These experiments are performed in large-scale fluid mechanics cycle tank of Wuhan University of technology, the wave test section of the cycle tank is 20 m in length, 2.7 m in width and 1.2 m in depth. The wave tank can produce regular waves with a period of 0.5~4 s, which satisfy the conditions of model tests.

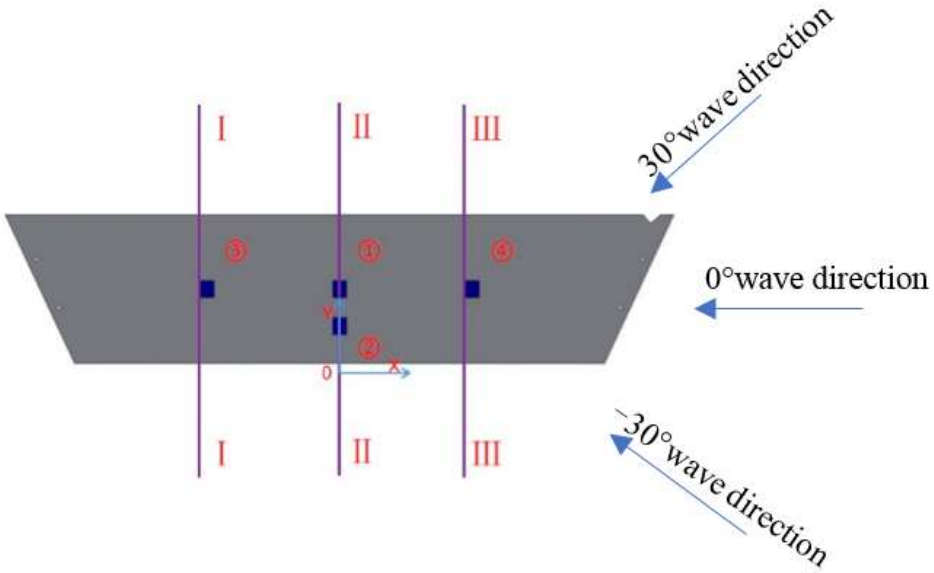

Figure 3. Measuring-points and wave directions.

2.3. Three-Dimensional Hydroelastic Method and Simulation Model

The relationship between motion and response of floating body in waves is linear; the coupled motion and displacement with deformation of the floating body can be expressed as follows:

$$u = \sum_{r=1}^{m} (u_r, v_r, w_r) p_r \tag{5}$$

where P_r (r = 1, 2, . . . , m) is the principal coordinate of the r order modal of floating body structure.

The structural stress response of large floating body can also be solved by the mode superposition principle. The total stress can be written as follow:

$$\sigma_x(x, y, z) = \sum_{r=1}^{m} p_r \sigma_{x,r} \tag{6}$$

The frequency domain equilibrium equation of the floating body can be written as follows:

$$\left\{-\omega_e^2([m] + [A]) - i\omega_e[B] + [k] + [C]\right\}\{\xi\} = \left\{F^{DI}\right\} \tag{7}$$

where $[m]$ is mass matrix structure, $[A]$ is hydrodynamic added mass matrix, $[B]$ is the hydrodynamic wave damping matrix, $[C]$ is hydrostatic restoring force matrix, $[k]$ is the stiffness matrix of structure, $\{\xi\}$ is the modal motion vector and $\{F^{DI}\}$ is the self-excited force of waves; the self-excited force of waves is obtained by integrating the incident potential and diffraction potential on wet surface, as shown in Equation (8).

$$\{F^{DI}\} = \left\{F^{F-K} + F^{D}\right\} = i\omega\rho \int\int_{S_B} (\phi_I + \phi_D) n_i dS \tag{8}$$

In Equation (8), each element of additional mass matrix [A] and wave damping matrix [B] can be obtained by integrating the radiation potential on wet surface, as shown in Equations (9) and (10):

$$A^{ij} = \rho \mathrm{Re}\left\{ \iint_{S_B} \varphi_R^j h^i n dS \right\} \tag{9}$$

$$B^{ij} = \rho \omega_e \mathrm{Im}\left\{ \iint_{S_B} \varphi_R^j h^i n dS \right\} \tag{10}$$

where, h^i is the modal function of the i-th order, A^{ij} is the element in the additional mass matrix and B^{ij} is the element in the additional damping matrix. The diffraction velocity potential and radiation velocity potential can be solved by the source and sink method on the basis of the boundary element method, as shown in Equation (11).

$$\varphi = \iint_{S_B} \sigma(x_h) G(x_h; x_s) dS \tag{11}$$

where $\sigma(x_h)$ is source intensity function. In this study, a hydrodynamic computing platform named Hydrostar is used to calculate each velocity potential and hydrodynamic coefficient. The time-domain structural response of the large floating body is obtained by the time-domain equilibrium equation of hydroelasticity, as shown in Equation (12).

$$([m] + [A^\infty])\left\{\ddot{\xi}(t)\right\} + ([k] + [C])\{\xi(t)\} + \int_0^t [K(t-\tau)]\left\{\dot{\xi}(\tau)\right\} d\tau = \left\{F^{DI}(t)\right\} \tag{12}$$

where [A^∞] is the additional mass matrix when the frequency is infinite and [$K(t)$] is the impact response function matrix.

HOMER software is a three-dimensional hydroelasticity solver developed by the French Classification Society which is used to conduct numerical simulation of the trapezoidal floating body [11]. The structure model and the hydrodynamic model should be established in HOMER, and the hydrodynamic pressure should be transferred between the structure model and the hydrodynamic model. The structural model and hydrodynamic model are shown in Figure 4. In the structural model, the basic size of the elements is 20 mm, with a total of 26,799 elements and 10,490 nodes. The deck of the structural model is made of 304 stainless steel, and the part below the deck is made of PVC foam. The material attribute parameters are measured by the two-point bending test, whose density is 30 kg/m^3, elasticity modulus is 0.3 Mpa and Poisson's ratio is 0.3. The basic size of the hydrodynamic model elements is 25 mm, with a total of 3017 elements and 2912 nodes.

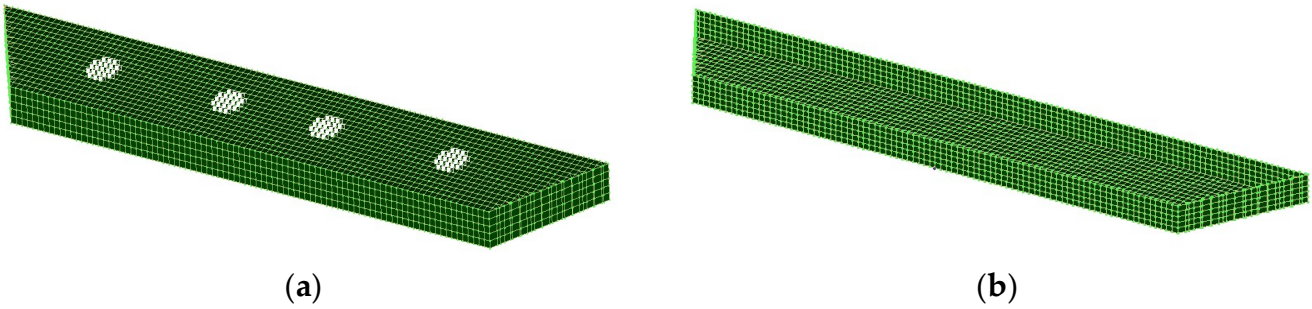

(**a**) (**b**)

Figure 4. Numerical simulation model. (**a**) Structural model. (**b**) Hydrodynamic model.

3. Results and Discussions

3.1. Modal Analysis

The modal superposition method is used to analyze the movement and response of the floating body by Homer. Firstly, modal analysis of the trapezoidal floating model must be carried out. The finite element solver Nastran and fluid-structure interaction analysis software Homer are used to calculate the dry and wet frequency of the trapezoidal floating model respectively. The fourth order flexible mode is described in Figure 5. The length of the model is larger than the width; therefore, it can be found that the modes are mainly composed of vertical vibration and torsion; the wet frequency of the structure is generally less than the dry frequency in the corresponding modes, as illustrated in Table 2.

Table 2. Dry/wet frequencies of the mode.

The Order of Flexible Mode	Dry Frequency (rad/s)	Wet Frequency (rad/s)
1	21.101	12.056
2	48.760	16.375
3	67.223	27.744
4	76.786	45.691

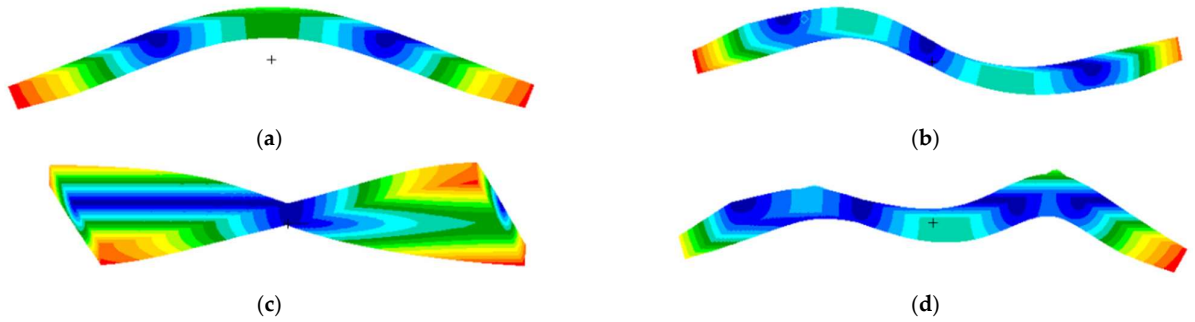

Figure 5. The schematic diagram of modal of a trapezoidal floating model. (**a**) The first order flexible mode. (**b**) The second order flexible mode. (**c**) The third order flexible mode. (**d**) The fourth order flexible mode.

3.2. Frequency Domain Response Analysis

In the experiments, the time history of the stress response of on the trapezoidal floating model is obtained. The time history of equivalent stress RAO at different wave directions and frequencies are compared with the calculation results. Figure 6 shows the time history of stress RAO of the measuring point No. 1, which is located in the middle of the ship. According to Figure 5a–c, it can be seen that there are multiple peaks in the time history of stress RAO under the three wave directions, the second peak usually occurs near the first order flexible mode of the trapezoidal floating model. The wave direction of 30° is close to that of −30° in the low-frequency region, the variability increases with frequency. According to Figure 5d, the peak value at 0°, 30° and −30° wave direction is close, and the peak value is the highest when the wave direction is 0°; the first peak value in the three wave directions appeared in the range of about 2 m which is closed to the length of the model. The corresponding wavelength of the first peak value in the wave direction 30° and −30 is shorter than that in the wave direction 0°, and the peak frequency is larger.

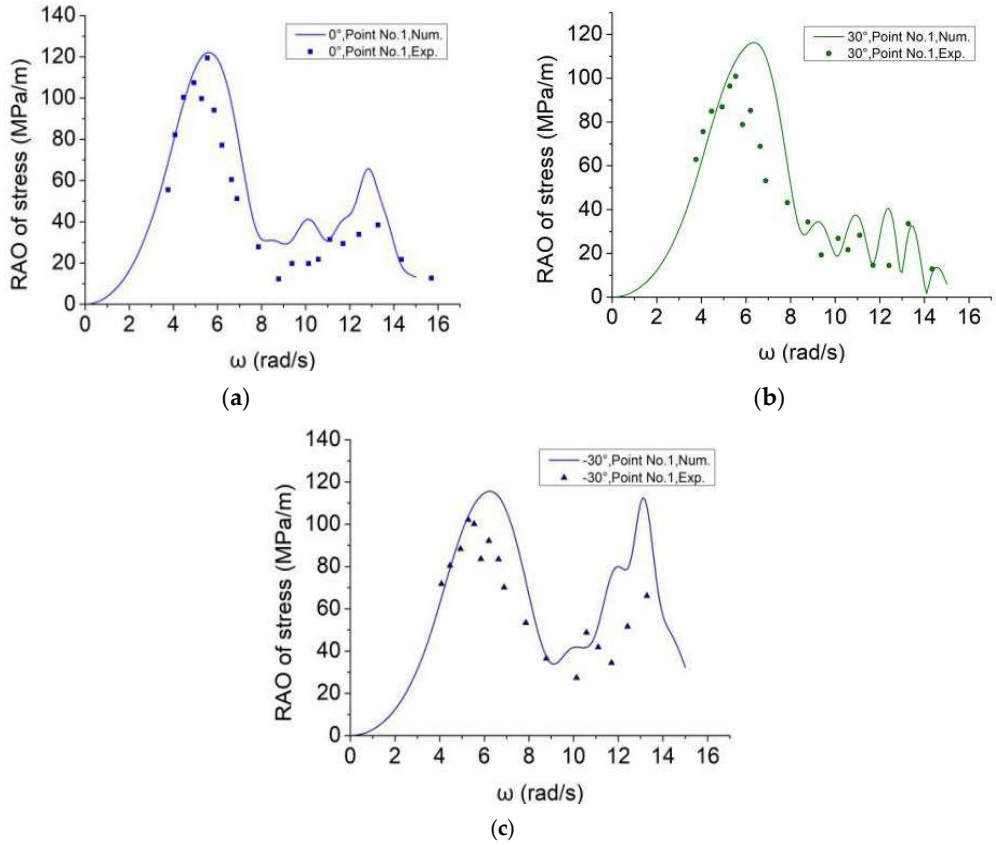

Figure 6. Frequency results of point 1. (**a**) Wave direction 0°. (**b**) Wave direction 30°. (**c**) Wave direction −30°.

An overview of experimental and numerical results from Figures 6 and 7 reveals that experiment and numerical results have close values. In the stage of high frequency, multi-peaks are appeared by numerical calculation in Figures 6 and 7. It is indicated that hydro-elastic responses are induced in stage of high frequency. It is found that the frequencies at multi-peaks are very close, so it is difficult to design experimental wave cases whose wave frequencies are just equal to the frequencies at RAO multi-peaks in simulation; experimental cases covering low and medium frequency-scope have close values to numerical calculations.

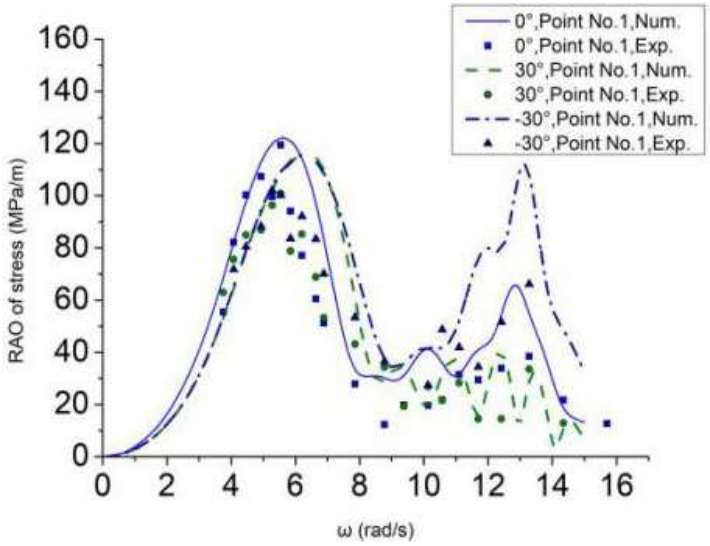

Figure 7. Frequency results of point 1 with wave direction 0°, 30° and −30°.

3.3. Time Domain Response Analysis

The time domain response of the trapezoidal floating model is obtained by the experimental date of the measuring point 1. Meanwhile, the time domain history of stress in the measuring point No. 1 is obtained by numerical simulation; the two results are compared and analyzed to study the time domain response characteristics of the trapezoidal floating model. Two time-domain conditions are selected, as shown in Table 3, to investigate the structural response under two wave frequencies. Figures 8 and 9 show the time domain calculation results of case 1 and 2, respectively. By comparing and analyzing the experiment results and simulation results in Figures 8 and 9, the time domain history of stress, the deformation mode and the relative position between the model and wave are generally the same, which verifies the validity of the experiment results and the simulation results.

Table 3. Wave conditions.

Case	Location	Frequency (rad/s)	Period (s)	Wave Height (mm)	Wave Direction (°)
1	1	5.540	1.134	80	0
2	1	12.417	0.506	80	0

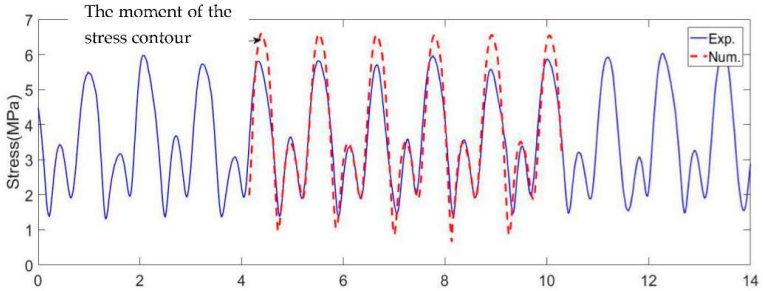

(**a**)

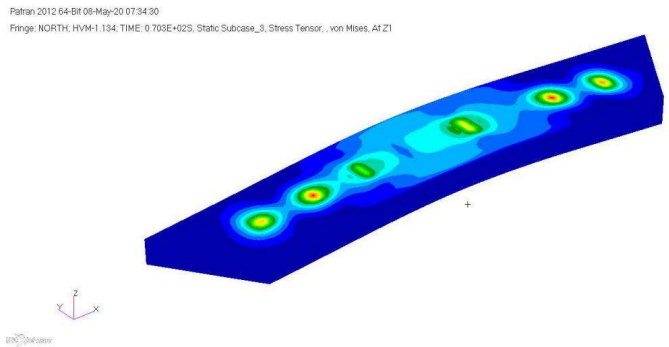

(**b**)

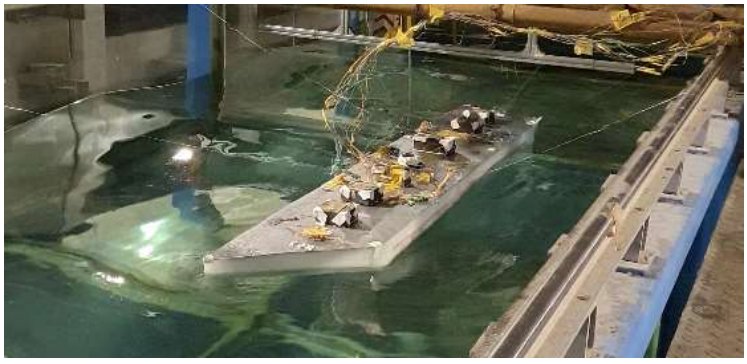

(**c**)

Figure 8. Result of Case 1. (**a**) The time domain history of stress in the measuring point No. 1 of case 1. (**b**) Stress contour at hogging of the case 1. (**c**) The experimental scene at hogging of the case 1.

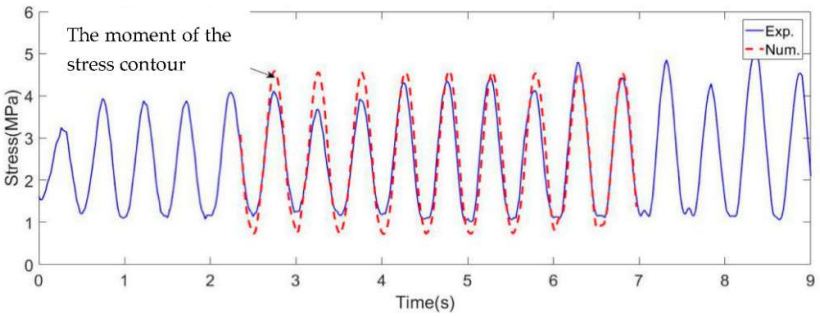

(**a**)

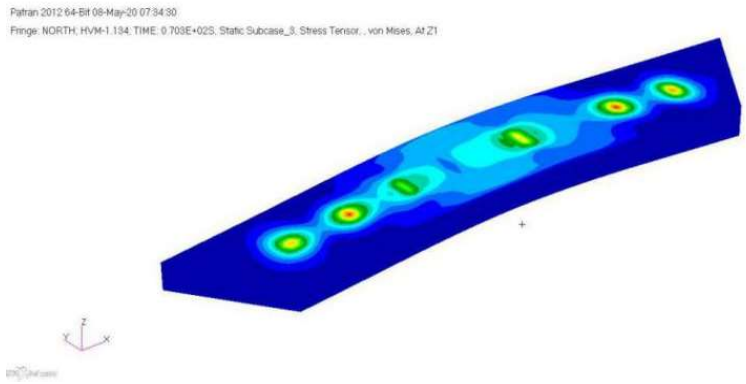

(**b**)

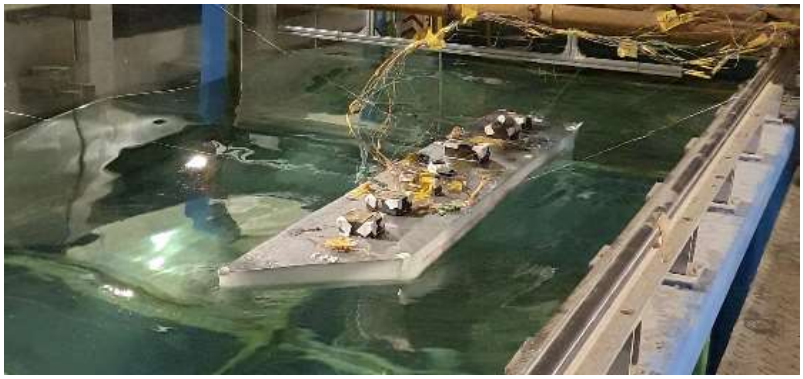

(**c**)

Figure 9. Result of Case 2. (**a**) The time domain history of stress in the measuring point No. 1 of case 2. (**b**) Stress contour at hogging of the case 2. (**c**) The experimental scene at hogging of the case 2.

The time domain stress history data relevant to case 1 and 2, based on results shown in Figures 8a and 9a, are analyzed and presented in the Figures 10 and 11, respectively. Figure 10 is the stress amplitude spectrum characteristic curve of measuring point 1 in case 1; it is seen that there are multi peak values in amplitude distribution. The first frequency of peak value is 5.378 rad/s, which is closed to the design frequency of case 1. The second and third frequency of peak value is 11.204 rad/s, 16.582 rad/s, respectively, which is 2 and 3 times of the first frequency of peak value. The second and the third peak frequency are very close to the first order and second order wet frequency of the model; the relationship between wet frequency and wave frequency is close to double, which reflects the characteristics of hydroelastic response clearly. Figure 10 shows the stress amplitude spectrum characteristic curve of measuring point 1 in case 2; it is found that there is only one peak value, the frequency of peak value 12.541 rad/s, which is close to the wave frequency, which means that the response of the model case 2 is mainly caused by the wave load. Hydroelastic response is not obvious, because when the wave frequency and the wet frequency of first order flexible modal is consistent, hydroelastic response will occur.

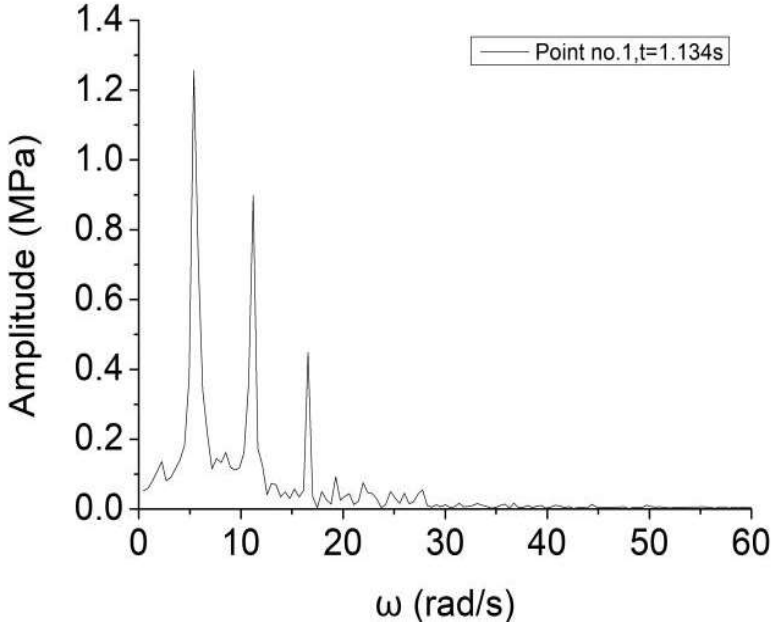

Figure 10. Stress amplitude spectrum of case 1.

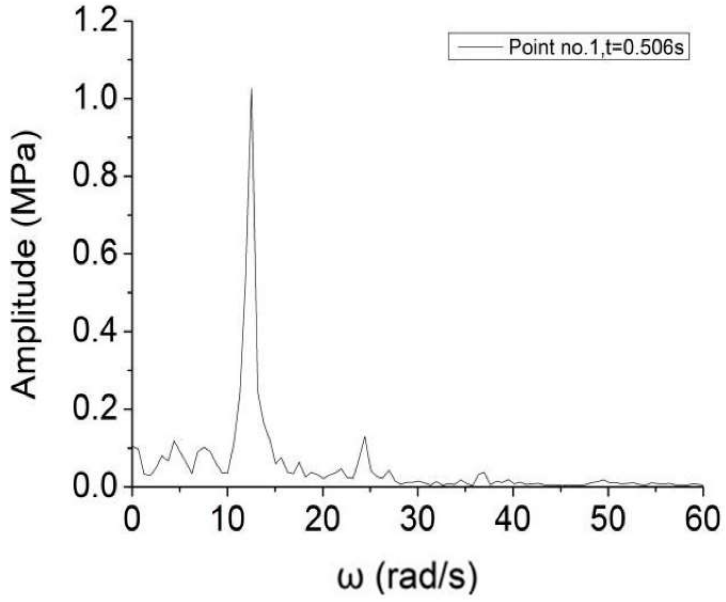

Figure 11. Stress amplitude spectrum of case 2.

4. Conclusions

In this paper, the response characteristics of a trapezoidal floating model are studied by experiments and three-dimensional hydro-elastic numerical solver. The experimental and simulation results are analyzed comprehensively and contrastively, and the following conclusions are obtained:

(1) With the comparison between the experimental and simulation results, it is found that the results are close matching at the beginning, which verifies the effectiveness of the experiment and simulation method adopted;

(2) The model is studied by experiment and numerical methods and the hydroelastic responses is generated. Frequency-domain RAOs of stress have multiple, significant and close peaks. The time-domain stress curves is transformed by Fourier transformation to analyze frequency-spectrum, indicating springing responses are induced. The hydro-elastic response should be considered in the design of platform.

(3) The time-domain stress curves of the experimental model increase with the wave period;
(4) Under some wave conditions, there is a large stress response of the model, which is worthy of designers' attention.

The response characteristics of a trapezoidal floating model are studied. Due to some structural differences between the model and the real structure, it is necessary to use the numerical simulation method to evaluate the structural response of the real trapezoidal platform structure.

Author Contributions: Conceptualization, W.L. and X.S.; methodology, W.L.; software, G.Z.; validation, W.L.; formal analysis, G.Z.; investigation, X.S.; resources, X.S.; data curation, X.S.; writing—original draft preparation, X.S.; writing—review and editing, X.S.; supervision, W.L. All authors have read and agreed to the published version of the manuscript.

Funding: This research was funded by the National Natural Science Foundation of China grant number No. 52101371 and No. 52071243 and National Defense Basic Research Program of China (No. JCKY2020206B037).

Data Availability Statement: Not applicable.

Conflicts of Interest: The authors declare no conflict of interest.

References

1. Rognaas, G.; Xu, J.; Lindseth, S.; Rosendahl, F. Mobile offshore base concepts: Concrete hull and steel topsides. *Mar. Struct.* **2001**, *14*, 5–23. [CrossRef]
2. Suzuki, H.; Harada, H.; Natsume, T.; Maeda, K.; Iijima, K.; Hayashi, T. Technical Challenge on VLFS in Japan after Mega-Float Project. In Proceedings of the ASME 2017 36th International Conference on Ocean, Offshore and Arctic Engineering, Trondheim, Norway, 25–30 June 2017. V009T12A013.
3. Suzuki, H. Overview of Megafloat: Concept, design criteria, analysis, and design. *Mar. Struct.* **2005**, *18*, 111–132. [CrossRef]
4. Song, B. *Research on the Connector of Very Large Floating Offshore Base*; Shanghai Jiao Tong University: Shanghai, China, 2012. (In Chinese)
5. Defense Science and Technology Industry Military-Civilian Integration Development Achievement Exhibition. *Mil. Ind. Cult.* **2015**, *12*. ISSN: 1674-1714 (In Chinese)
6. Yago, K.; Hara, S. On the Hydroelastic Response of Box-Shaped Floating Structure with Shallow Draft (Tank Test with Large Scale model). *J. Jpn. Soc. Nav. Archit. Ocean. Eng.* **1996**, 341–352. [CrossRef]
7. Yago, K.; Endo, H. Model Experiment and Numerical Calculation of the Hydoelastic Behavior of Matlike VLFS. In Proceedings of the 2nd International Workshop on Very Large Floating Structure, Hayama, Japan, 25–28 November 1996; pp. 209–216.
8. Wu, Y.S.; Ding, J.; Li, Z.W.; Ni, X. Hydroelastic responses of VLFS deployed near islands and reefs. In Proceedings of the 36th International Conference on Ocean, Offshore and Arctic Engineering (OMAE), Trondheim, Norway, 25–30 June 2017.
9. Chen, G.; Yang, J.; Zhang, C. Experimental research on hydroelasticity on box-typed flexible VLFS in waves. *Ocean. Eng.* **2003**, *21*, 1–5. (In Chinese)
10. Wan, Z. *Numerical Analysis and Experimental Study on Hydroelasticity of Super-Large Floating Body*; Dalian University of Technology: Dalian, China, 2014. (In Chinese)
11. Bishop, R.E.D.; Price, W.G. *Hydroelasticity of Ships*; Cambridge University Press: Cambridge, UK, 1979.
12. Wu, Y. Hydroelasticity of Floating Bodies. Ph.D. Thesis, Brunel University, Brunel, UK, 1984.
13. Ohkusu, M.; Namba, Y. Analysis of Hydroelastic Behavior of a Large Floating Platform of Thin Plate Configuration in Waves. In Proceedings of the International Workshop on Very Large Floating Structures, Hayama, Japan, 25–28 November 1996; pp. 143–148.
14. Hamamoto, T.; Sekine, S. Simplified equation for estimating added mass distribution over large floating structures. In Proceedings of the ISOPE2000, Seattle, WA, USA, 28 May–2 June 2000; pp. 57–64.
15. Mamidipudi, P.; Webster, W.C. *The Motions Performance of a Mat-Like Floating Airport*; ICHMT'94; TU Delft Library: Delft, The Netherlands, 1994; pp. 363–375.
16. Malenica, S.; Sireta, F.X.; Bigot, F.; Wang, C.; Chen, X.B. Some aspects of hydro structure coupling for combined action of seakeeping and sloshing. In Proceedings of the OMAE Conference, Honolulu, HI, USA, 31 May–5 June 2009.
17. Lu, Y.; Zhou, Y.; Fan, C.; Zhang, Z.; Tian, C. Hydroelasticity of floating platform near island effected by bathymetry based on THAFTS software. *Ship Mech.* **2019**, *5*, 602–610. (In Chinese)
18. Zhang, G.; Liu, W.; Wu, W.; Song, X.; Wang, S. 3D Hydorelastic Study of A Trapezoidal Large Floating Structure. In Proceedings of the International Society of Offshore and Polar Engineers, Hawaii, USA, 16–21 July 2019.
19. Yang, P.; Gu, X. Motion responses of floating structures near small islands. *Ship Mech.* **2017**, *21*, 152–158. (In Chinese)
20. Yang, P.; Gu, X. Analysis on the hydroelastic responses and structural strength of VLFS module. *Ship Mech.* **2015**, *19*, 553–565. (In Chinese)

21. Zhou, Y.; Ding, J.; Tian, C.; Zhang, Z.; Ling, H.; Wang, D. Hydrodynamic analysis of floating platform considering effect of complicated seabed near islands and reefs. *Ship Eng.* **2018**, *A1*, 280–286. (In Chinese)
22. Tian, C.; Ding, J.; Yang, P. Prediction of dynamic responses of floating structures under wave environment near islands and reefs. *Ship Mech.* **2014**, *18*, 1284–1291. (In Chinese)
23. Selvan, S.A.; Ghosh, S.; Behera, H.; Meylan, M. Hydroelastic response of a floating plate on the falling film: A stability analysis. *Wave Motion* **2021**, *104*, 102749. [CrossRef]
24. Selvan, S.A.; Gayathri, R.; Behera, H.; Meylan, M. Surface wave scattering by multiple flexible fishing cage system. *Phys. Fluids* **2021**, *33*, 037119. [CrossRef]
25. Selvan, S.A.; Behera, H. Wave energy dissipation by a floating circular flexible porous membrane in single and two-layer fluids. *Ocean. Eng.* **2020**, *206*, 107374. [CrossRef]
26. Behera, H.; Ng, C.-O.; Sahoo, T. Oblique wave scattering by a floating elastic plate over a porous bed in single- and two-layer fluid systems. *Ocean. Eng.* **2018**, *159*, 280–294. [CrossRef]